MRS Communications (2024) 14:1113–1126
© The Author(s), 2024
https://doi.org/10.1557/s43579-024-00673-x

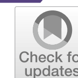

Van der Waals magnetic materials for current-induced control toward spintronic applications

Jeongchun Ryu, Shivam Nitin Kajale, and Deblina Sarkar, MIT Media Lab, Massachusetts Institute of Technology, Cambridge, MA 02139, USA
Address all correspondence to Deblina Sarkar at **deblina@mit.edu**

(Received 20 July 2024; accepted 18 October 2024; published online: 11 November 2024)

Abstract
Spintronics, leveraging electron spin for information processing, promises substantial advancements in energy-efficient computing. Van der Waals (vdW) magnetic materials, with their unique-layered structures and exceptional magnetic properties, have emerged as pivotal components in this field. This report explores the current-based control of vdW magnets, focusing on the spin–orbit torque (SOT) mechanism, which is crucial for spintronic applications. Key studies on Fe_3GaTe_2/Pt and Fe_3GaTe_2/WTe_2 heterostructures are highlighted, demonstrating efficient SOT switching at room temperature. The advantages of vdW magnets for SOT switching, including high spin-torque efficiencies and superior interface quality, are discussed. The report also examines future directions, such as wafer-scale growth techniques, materials design for enhanced Curie temperatures (T_c), and the development of magneto tunnel junctions using all-vdW materials. These advancements underscore the potential of vdW magnetic materials in developing scalable, high-performance spintronic devices, paving the way for significant breakthroughs in energy-efficient computing.

Introduction
The rapid advancement of spintronics, which exploits the electron's spin for computation, in addition to its charge, has paved the way for revolutionary changes in the development of energy-efficient computing technologies.[1,2] Central to these advancements are van der Waals (vdW) magnetic materials, characterized by their unique-layered structures held together by weak van der Waals forces.[3,4] These materials show significant promise in enhancing the performance and miniaturization of spintronic devices due to their ability to maintain magnetic properties down to the monolayer limit.[5]

Recent breakthroughs have highlighted the intrinsic ferromagnetism in two-dimensional (2D) vdW materials such as CrI_3, $Cr_2Ge_2Te_6$, and Fe_3GeTe_2, which exhibit robust magnetic ordering even when exfoliated to a single layer.[6–8] These properties make vdW materials highly attractive for developing next-generation, low-power, and high-density magnetic memory and logic devices. The discovery of intrinsic ferromagnetism in Fe_3GaTe_2 with a high T_c (up to 380 K) and a large perpendicular magnetic anisotropy (PMA) has been particularly noteworthy, positioning it as a leading candidate for spintronic devices that operate efficiently at room temperature.[9]

On the other hand, current-induced magnetization switching mechanisms, like spin-transfer torque and spin–orbit torque (SOT), have emerged as critical techniques for achieving rapid, scalable, and energy-efficient control of spintronic devices.[10–12] SOT offers several advantages for spintronic devices including reduced switching currents, quicker response times without a short incubation period, and longer device lifespans due to the separation of the high current write path from the magnetic tunnel junction (MTJ) body. The advent of 2D magnetic materials has opened new pathways for low-current, highly efficient SOT applications. They offer perfectly smooth interfaces for optimal interaction with spin–orbit coupling materials, thereby increasing the efficiency of SOTs. Moreover, these materials can be effectively combined with the vdW topological materials that exhibit spin-momentum locking, promising significantly greater SOT efficiencies and the possibility of switching magnetization without an external magnetic field. Building on this foundation, recent studies have demonstrated significant advancements in achieving field-free, deterministic switching of magnetization above room temperature in vdW materials.

This prospective report aims to provide a comprehensive overview of the current state of research in current-based control of vdW magnetic materials, discuss the mechanisms enabling such control, and explore the prospects for these materials in energy-efficient computing. By synthesizing findings from recent studies with other significant advancements in the field, this report will outline the potential pathways for realizing scalable and commercially viable spintronic devices using vdW magnetic materials. The report is structured as follows: the next section discusses the mechanisms of current-based control of vdW magnets, focusing on SOTs and their role in current-induced switching in materials with perpendicular magnetic anisotropy (PMA). Following this, we provide a comprehensive survey of recent advances in current-based control of vdW ferromagnets, highlighting key studies on materials such as Fe_3GaTe_2 and their integration with heavy metals and low-symmetry vdW materials

Jeongchun Ryu and Shivam Nitin Kajale have equally contributed this work.

for efficient spintronic applications. Finally, the last section explores the prospects for vdW magnets-based spintronics, highlighting the need for wafer-scale growth, materials' design strategies for enhancing T_c, current-based control of magnetic anisotropy, prospects for voltage and strain-assisted switching, and the development of magnetic tunnel junctions (MTJs) using all-vdW materials.

Mechanisms of current-based control of vdW magnets

Spin–orbit torques and current-induced switching in perpendicular magnetic anisotropy materials

Current-induced SOTs have emerged as a robust mechanism for controlling ferromagnetic materials (FM), essential for the advancement of spintronic devices.[13–16] The SOTs originate from spin–orbit interactions, primarily facilitated by the spin-Hall effect,[17] the Rashba-Edelstein effect[18] and reduced crystal symmetry. There are two principal types of SOTs: damping-like torque and field-like torque. The damping-like torque $\tau_{DL,y}$, mainly reported in heavy metal (e.g., Pt, Ta, and W)[15,16] acts perpendicularly to both the magnetization m and the direction of the injected spin-polarized current σ_y; thus, $\tau_{DL,y}$ can be expressed as $m \times (\sigma_y \times m)$. Here, we assume that the electrical current is applied along x-direction and σ_y is generated along y-direction. $\tau_{DL,y}$ is highly effective in the deterministic switching of the magnetization direction since $\tau_{DL,y}$ is analogous to the Gilbert damping in magnetization dynamics. Conversely, the field-like torque $\tau_{DL,y}$ operates similarly to an effective magnetic field that aligns with the spin polarization direction σ_y. $\tau_{FL,y}$ contributes to the precessional motion of the magnetization and is described by $m \times \sigma_y$. Although the $\tau_{FL,y}$ is generally less efficient in achieving magnetization switching compared to the damping-like torque, it plays an essential role in modifying the effective magnetic field experienced by the magnetization.[19,20] Recently, in the material systems which have low-symmetry crystals, out-of-plane damping-like torque $\tau_{DL,z}$ of the form of $m \times (\sigma_z \times m)$ is reported when the current is applied along the low-symmetry crystal axis (Fig. 1). Low-symmetry transition-metal dichalcogenides (TMDs), which consist of a transition-metal atom (e.g., Mo, W) and a chalcogen atom (e.g., S, Se, or Te), are representative materials.[21,22] Generation of $\tau_{DL,z}$ is also reported in collinear[23,24] and non-collinear antiferromagnets[25,26] and altermagnets.[27] Similarly, field-like torque $\tau_{FL,z}$ induced by $\sigma_z \propto m \times \sigma_z$ and damping-like torque $\tau_{DL,x}$ due to σ_x also reported ($\propto m \times (\sigma_x \times m)$).[28] The total SOTs could be expressed in Eq. 1:

$$\tau_{SOT} = \tau_{DL,y} m \times (\sigma_y \times m) + \tau_{FL,y} m \times \sigma_y + \tau_{DL,z} m \times (\sigma_z \times m) + \tau_{FL,z} m \times \sigma_z + \tau_{DL,x} m \times (\sigma_x \times m), \quad (1)$$

where $\tau_{DL,y}$, $\tau_{FL,y}$, $\tau_{DL,z}$, $\tau_{FL,z}$, and $\tau_{DL,x}$ are SOT coefficient of $\tau_{DL,y}$, $\tau_{FL,y}$, $\tau_{DL,z}$, $\tau_{FL,z}$ and $\tau_{DL,x}$, respectively.

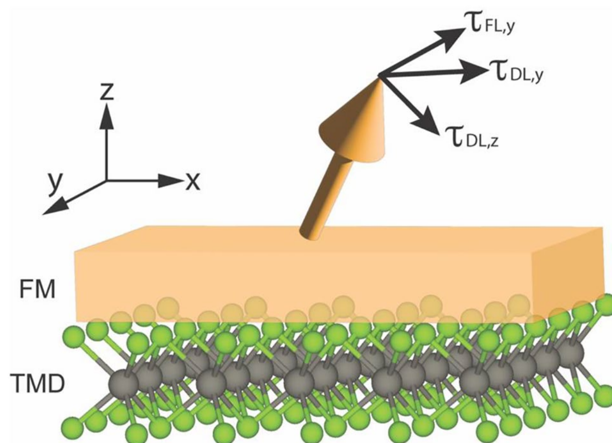

Figure. 1. Schematic illustration of SOTs in FM/TMD bilayers. Orange arrow represents the m of ferromagnet (FM). Here, we illustrate $\tau_{DL,y}$, $\tau_{FL,y}$, and $\tau_{DL,z}$ in black arrows. Note that other SOT components could be also obtained in the similar manner shown in Eq. 1.

For the practical memory device application, ferromagnets with PMA offer advantages over those with in-plane anisotropy.[29] Devices employing in-plane magnetization switching encounter inherent limitations, such as constraints on device shape and size to maintain the large in-plane anisotropies, and prolonged switching times caused by slow incubation. On the other hand, PMA enhances not only thermal stability, a key factor in maintaining data integrity at smaller scales but allows for the reduction of magnetic volume without compromising stability.[29] In particular, interfacial PMA, originated in Fe-alloy/oxide layer, is essential for scaling down devices to sub-nm dimensions, thus, increasing data storage density.[30] In addition, $\tau_{DL,y}$ acting on ferromagnet with PMA significantly decreases incubation time since m and σ_y are orthogonal, leading to ultrafast switching[19] in SOT systems. However, interfacial PMA in metallic films is strongly dependent on substrate properties and interface quality.[31] For maintaining an atomically smooth interface and minimal intermixing, recently two-dimensional vdW ferromagnetic materials have been extensively investigated.[3,6–8,32,33] The vdW ferromagnets predominantly exhibit an intrinsic magneto-crystalline anisotropy, which arises from the reduced crystal symmetry of their layered structures. This property enables to retain its magnetic anisotropy in monolayer state.[6,7] The vdW ferromagnets with PMA, especially operating above room temperature, offer crucial advantage to harness the capabilities.[8,9]

While SOTs present significant advantages in spintronic applications, they also pose certain challenges, particularly in systems with PMA. A primary issue is the necessity of an in-plane external field for the deterministic switching of perpendicular magnetization.[13,14,19] Specifically, with magnetization along the z-axis, effective fields of $\tau_{DL,y}$ and $\tau_{FL,y}$, which we can typically expect in conventional heavy metal/ferromagnet bilayer, exhibit rotational and mirror symmetry relative to the xz and xy-planes, respectively.[15,16] This prevents switching

by the injected current alone. Consequently, an in-plane field along the x-axis is essential to disrupt this symmetry. To this end, implanting a local symmetry breaking mechanism which operates inside the material systems is imperative. Many recent progresses have been reported in conventional metallic system to break the symmetry: exchange-biased field from antiferromagnet,[34,35] interlayer exchange coupling,[36,37] or magnetic trilayer consisting of in-plane and perpendicular ferromagnetic layers,[20,38] tilted anisotropy of the nanomagnet,[39,40] spin anomalous Hall effect in ferromagnet,[41,42] lateral inversion asymmetry,[43] and interplay of SOT and spin-transfer torque.[44] Most of the introduced mechanisms involve intricate multilayer structures [34–38,41,42] or complicated shape engineering[39,40,43] that pose challenges toward scalability. A simpler proposition is to use SOT materials with low-symmetry, which can intrinsically generate the out-of-plane damping-like torque, $\tau_{DL,z}$, for field-free switching of PMA magnets [21–28,33].

Characterization of SOTs and current-induced magnetization switching

The harmonic Hall measurement and spin-torque ferromagnetic resonance (ST-FMR) techniques are widely employed for the quantitative analysis of SOTs. The lock-in harmonic Hall voltage measurement probes the oscillation of magnetization at its equilibrium position induced by the injected a.c. current of a few kHz.[15,16,45] The harmonic responses, influenced by the direction of the applied external magnetic field, allow for the characterization of each SOT component. This measurement technique is applicable to ferromagnets with both PMA and in-plane anisotropy. In ferromagnets with strong PMA, the harmonic Hall signal is typically obtained by sweeping the magnetic field along the x- and y-directions.[15,16] For ferromagnets with in-plane anisotropy or relatively weak PMA, the harmonic Hall signal is measured as a function of the azimuthal angle (ϕ) in the xy-plane under a specific magnetic field that maintains a single magnetic domain state.[22,32,45,46] Figure 2(a–c) illustrates representative first and second harmonic Hall resistance in a low-symmetry material system ($MnPd_3$/CoFeB). The obtained second harmonic resistance $R^{2\omega}$ can be expressed as follows:

$$R^{2\omega} = (R_0 - R^{2\omega}_{DL,y}\cos\phi + R^{2\omega}_{FL,y}\cos 2\phi\cos\phi + R^{2\omega}_{DL,z}\cos 2\phi + R^{2\omega}_{DL,x}\sin\phi + R^{2\omega}_{PNE}\sin 2\phi. \quad (2)$$

Here, the resistances $R^{2\omega}_{DL,y}$, $R^{2\omega}_{FL,y}$, $R^{2\omega}_{DL,z}$, and $R^{2\omega}_{DL,x}$ are associated with the SOT components $\tau_{DL,y}$, $\tau_{FL,y}$, $\tau_{DL,z}$, and $\tau_{DL,x}$. R_0 and $R^{2\omega}_{PNE}$ indicate device offset and anomalous Nernst resistance. By analyzing ϕ dependence based on Eq. (2), each SOT component can be quantitatively estimated.

ST-FMR measurement employs a radiofrequency (RF) current, with a typical frequency of a few GHz, to excite magnetization.[21,47] The RF current is applied along the x-axis, while an in-plane magnetic field is applied at a certain angle to the current. The spin current generated by the RF charge current exerts oscillating SOTs on the ferromagnet. Simultaneously, the anisotropic magnetoresistance of ferromagnet also oscillates at the same frequency, producing the rectified voltage signal V_{mix}. This signal is composed of the symmetric and antisymmetric Lorentzian functions F_S and F_A, i.e., $V_{mix} = V_S F_S + V_A F_A$, where the symmetric and antisymmetric voltage components are

$$V_S = \sin 2\phi (S_0 + S_1 \cos\phi),$$

$$V_F = \sin 2\phi (A_0 + A_1 \cos\phi).$$

Here, ϕ indicates the azimuthal angle between the RF current and the applied field. S_0 and A_0 are related to $\tau_{FL,y}$ and $\tau_{DL,z}$. S_1 and A_1 are associated with $\tau_{DL,y}$ and $\tau_{FL,z}$. Thus, analyzing V_S and V_A enables determination of each component of SOTs. Figure 2(d–f) indicates representative ST-FMR results obtained in $TaIrTe_4$/NiFe.[47] This method is typically applied to in-plane magnetization systems.

In addition to the aforementioned techniques, the anomalous Hall loop shift measurement is also utilized for characterizing the $\tau_{DL,z}$.[48] The anomalous Hall signal exhibits a shift that depends on the magnitude of the applied d.c. current, providing a direct measure of the out-of-plane effective magnetic field [Fig. 2(g, h)].

In the presence of spin–orbit torques (SOTs), magnetization switching can be demonstrated by injecting electrical currents.[13,14] This process typically involves sequentially injecting pulsed currents while gradually increasing the amplitude of each pulse. The critical current (or current density) is identified from the resulting current-swept magnetization switching curves at the point where the up-magnetization and down-magnetization signals average. In the absence of symmetry breaking, where $\tau_{DL,y}$ and $\tau_{FL,y}$ are dominantly observed in heavy metal/ferromagnet bilayers, an external magnetic field along the current direction is required for deterministic switching. However, in material systems with symmetry breaking, field-free switching can be observed. The most common method for current-induced magnetization switching is the anomalous Hall effect (AHE) measurement in crossbar-shaped devices as shown in Fig. 2(g, i). The magneto-optical Kerr effect[49] is also widely used, and it has been shown that switching can occur in a few picoseconds via the thermally activated helicity-independent all-optical switching mechanism,[50] whereas in AHE, incubation delays can extend switching times to a few hundred picoseconds.[19] It is important to note that magnetization switching results from the interplay of all SOT components, along with thermal fluctuations and the stochastic nature of domain wall nucleation. Consequently, determining the specific magnitude of each SOT component based solely on the switching current is challenging.

Recent advances in current-based control of vdW ferromagnets

The field of spintronics is experiencing remarkable advancements through the incorporation of vdW magnetic materials, reinvigorating the promise for energy-efficient and

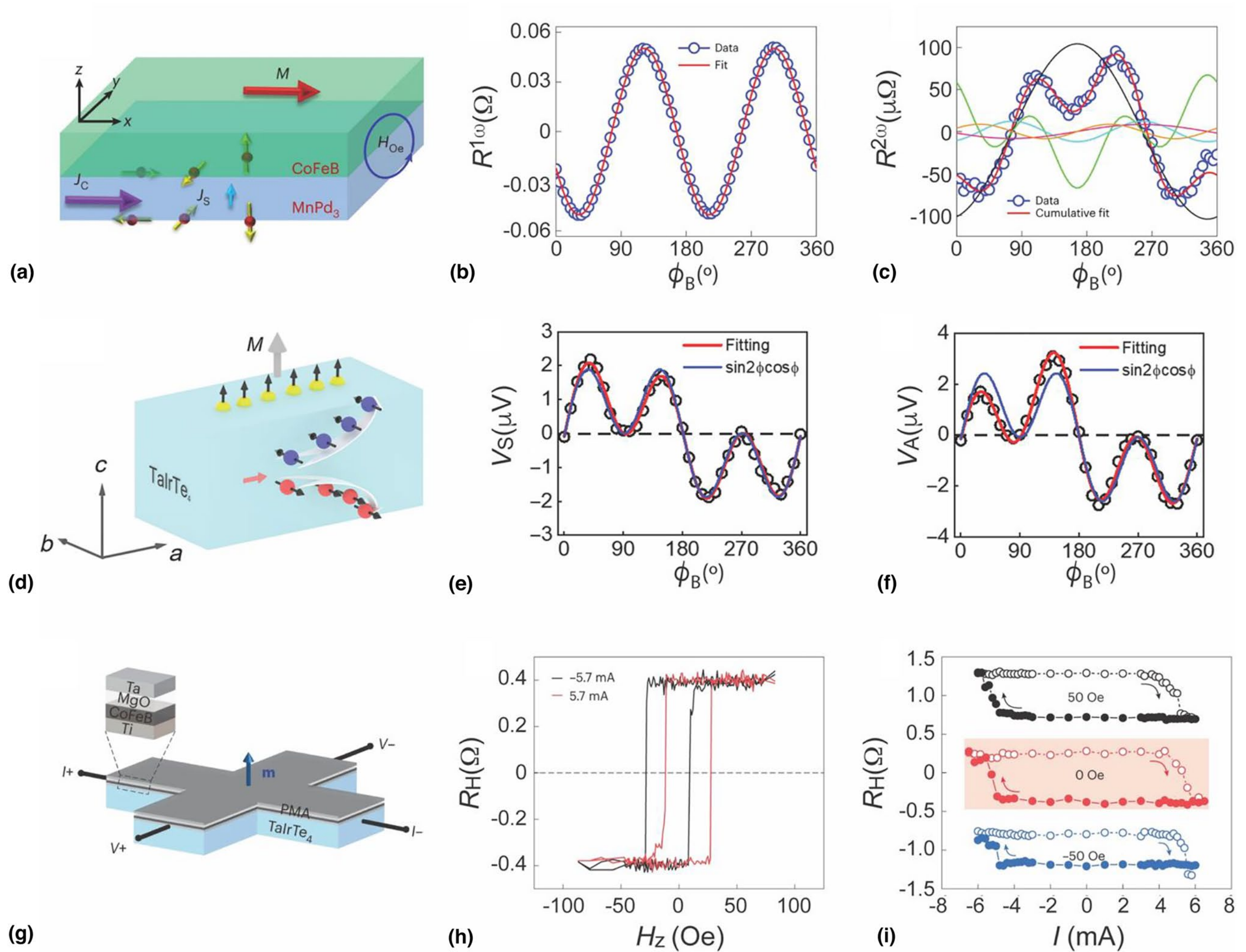

Figure. 2. Characterization of SOTs and current-induced switching (a) Schematic illustration of the CoFeB/$MnPd_3$ bilayer device. J_c, J_s, and H_{Oe} represent charge current density, spin current density, and Oersted field, respectively. (b, c) First and second harmonic resistance $R^{1\omega}$ and $R^{2\omega}$ as a function of azimuthal angle f_B. In (c), the pink, black, cyan, green, and orange lines represent the contribution of $\tau_{DL,x}$, $\tau_{DL,y}$, $\tau_{DL,z}$, $\tau_{FL,x}$ and $R^{2\omega}_{PNE}$, respectively. Copyright © 2023, Mahendra DC et al. [46] (d) Schematic of spin current accumulation under a current along the a-axis of $TaIrTe_4$. (e, f) ST-FMR signals of symmetric (e) and antisymmetric (f) components depending on f_B obtained in $TaIrTe_4$/NiFe. Copyright © 2024, Zhang et al. [47] (g) Schematic of $TaIrTe_4$/Ti/CoFeB/MgO/Ta Hall bar structure. (h) The shift of anomalous Hall loop under a d.c. current of 5.7 mA (red line) and – 5.7 mA (black line). (i) Current-induced magnetization switching obtained in different external magnetic fields. Copyright © 2023, Liu et al. [48].

high-density spintronic devices. Among other things, vdW magnetic materials offer significant advantages for SOT switching devices. Their unique-layered structure enables these materials to be thinned down to monolayers while broadly retaining their magnetic properties which facilitates the creation of ultra-thin, high-performance, energy-efficient devices. vdW materials ensure superior interface quality in heterostructures due to their atomically flat surfaces and minimal interlayer diffusion of atomic species. This can enhance spin transparency and result in efficient spin transfer across interfaces to reduce scattering and energy loss and improve device performance. Moreover, these materials can be seamlessly combined with emerging spin-momentum locking vdW topological materials to enhance SOT efficiencies and achieve performance levels exceeding those of heavy metals. Such heterostructure devices can also enable the field-free switching of PMA magnetization.

The first demonstration of SOT-induced switching in vdW magnetic materials occurred in bilayer systems of the metallic vdW ferromagnet Fe_3GeTe_2, which exhibits a strong PMA, and the heavy metals Pt and Ta. In the study by Alghamdi et al., thin Pt films (5 nm) sputtered on exfoliated Fe_3GeTe_2 flakes (15–23 nm) were patterned into Hall bar geometries.[51] The anomalous Hall effect tracked the ferromagnet's magnetization state, achieving non-volatile switching of out-of-plane magnetization at a threshold current of 2.5×10^7 A cm^{-2} at 180 K, in the presence of a symmetry breaking in-plane magnetic field. Similar experiments in Fe_3GeTe_2/Pt and Fe_3GeTe_2/Ta bilayer

systems by Wang et al. confirmed ferromagnet switching in both systems.[52] A given current drive was found to favor opposite magnetization states in Pt and Ta-based devices due to their opposite spin-Hall angles, further supporting the role of current-induced SOT in these systems. Topological insulators (TIs) are gaining attention as SOT layers in current-induced ferromagnet switching systems. TIs showcase spin-polarized Dirac surface states, leading to large spin-Hall angles. When an electric field is applied, the Rashba-Edelstein effect causes non-equilibrium spin accumulation, which exerts torque on the adjacent ferromagnet. Using the topological insulator $(Bi_{(1-x)}Sb_x)_2Te_3$ as a spin-Hall layer, Fujimura et al. successfully demonstrated non-volatile magnetization switching in epitaxially grown $Fe_3GeTe_2/(Bi_{(1-x)}Sb_x)_2Te_3$ stacks.[53] At 180 K, the threshold current density for switching a 6 nm Fe_3GeTe_2 film was 1.7×10^6 A cm^{-2} when a 100 mT in-plane magnetic field was applied. While such studies consistently exemplified the efficacy of vdW ferromagnets-based SOT switching systems, they were all limited by operation only at cryogenic temperatures, up to 200 K.

A study by Kajale et al. demonstrated the possibility of current-induced magnetization switching in Fe_3GaTe_2 above room temperature, when integrated with platinum (Pt) as a spin–orbit coupling layer.[32] Fe_3GaTe_2 is a metallic, vdW ferromagnet that exhibits a high T_c (~350 K) and strong perpendicular magnetic anisotropy (4.8×10^5 J m^{-3}), making it a credible candidate for vdW spintronics.[9] It is structurally similar to Fe_3GeTe_2, but showcases a T_C bump of ~150 K upon swapping the Ge with Ga. This has been attributed to the ferromagnetic exchange coupling between Fe atoms within the same atomic planes in Fe_3GaTe_2, as compared to Fe_3GeTe_2 where the in-plane exchange coupling between Fe atoms is antiferromagnetic, leading to spin frustration and a reduced T_C.[54] In the study by Kajale et al., the bilayer stack comprising Fe_3GaTe_2 and Pt was patterned into Hall bar geometry [Fig. 3(a)] and the magnetization state of the Fe_3GaTe_2 in response to current pulses was probed through anomalous Hall resistance measurement.[32] Deterministic and non-volatile switching of PMA magnetization in Fe_3GaTe_2 was achieved using a nominal in-plane field of 100 Oe with threshold switching current density as low as 1.69×10^6 A cm^{-2} at 300 K, as shown in Fig. 3(b). This marked the lowest switching current density among all previous vdW magnet-based SOT switching systems, including those operating below room temperature, highlighting the strong prospects of the Fe_3GaTe_2/Pt system

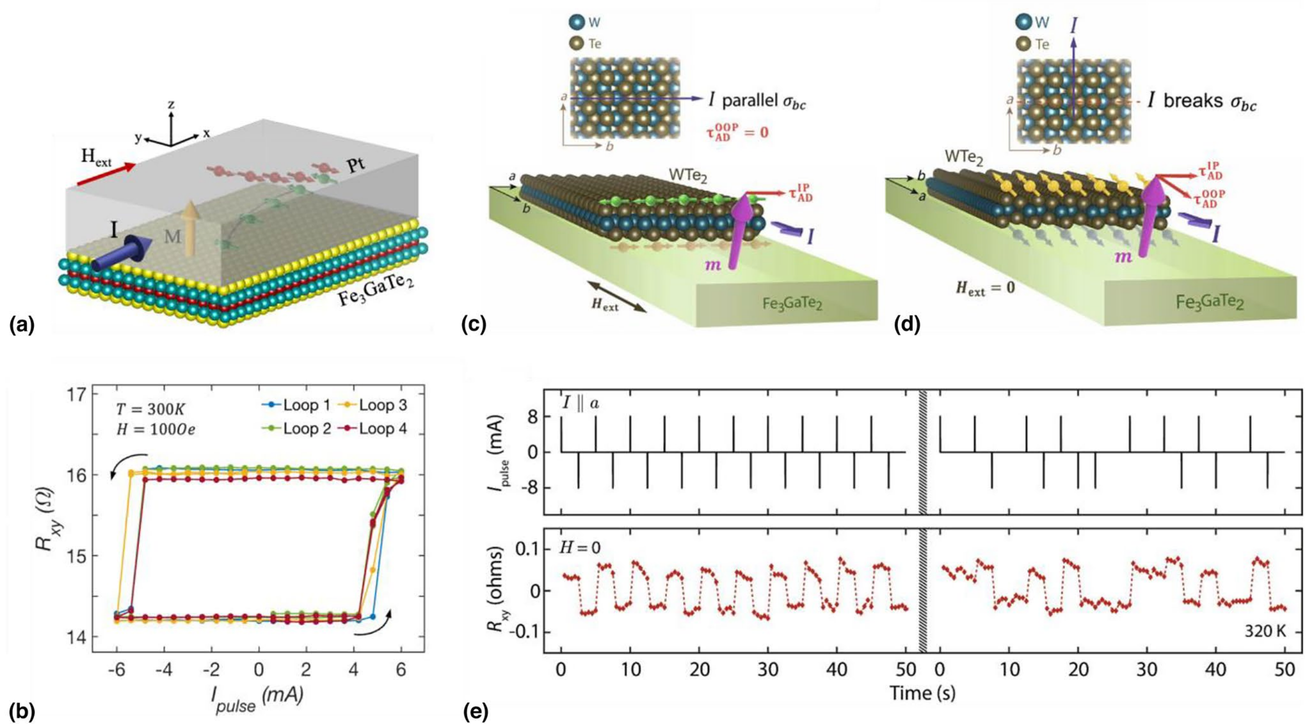

Figure. 3. Current-based control of the vdW ferromagnet Fe_3GaTe_2. (a) Schematic illustration of the Fe_3GaTe_2/Pt bilayer device, with directions of applied current and magnetic fields denoted. (b) Current-induced switching of PMA magnetization of Fe_3GaTe_2 at 300 K and 100 Oe field, recorded as anomalous Hall resistance. Four consecutive current pulsing cycles are presented. Copyright © 2024, Kajale et al. [32] (c, d) Schematic illustration of the Fe_3GaTe_2/WTe_2 heterostructure device, for current applied along the different crystallographic axes of WTe_2. A non-zero out-of-plane anti-damping torque, $\tau_{AD}^{OOP} = \tau_{DL,z}$is generated only when current is applied along the low-symmetry *a*-axis. (e) Deterministic and non-volatile switching of PMA magnetization in Fe_3GaTe_2 in response to a train of current pulses, at 320 K and without any external magnetic field. Copyright © 2024, Kajale et al. [33].

for energy-efficient spintronics. The low switching current density also allowed for the switching to be observed up to 320 K, quite close to the T_c of exfoliated Fe_3GaTe_2 (~ 328 K), due to reduced heating. The anti-damping-like SOT efficiency of the Fe_3GaTe_2/Pt system was estimated to be 0.093, close to the commonly observed value of ~ 0.1 in Pt-based systems, using field angle-dependent second harmonic Hall measurements.

In a similar vein, the work by Li et al. has explored the capabilities of Fe_3GaTe_2/Pt heterostructures[55] where the perpendicular magnetization of Fe_3GaTe_2 can be effectively switched at room temperature with a current density of 1.3×10^7 A cm^{-2}. This was achieved through spin–orbit torques in the Fe_3GaTe_2/Pt bilayer. The high SOT efficiency of approximately 0.28, quantitatively determined by harmonic measurements, was noted to be higher than that in Pt-based heavy metal/conventional ferromagnet devices. Yun et al. have also studied this system and reported a switching current density of 4.8×10^6 A cm^{-2} at room temperature.[56] Furthermore, they found that sputtering Pt on Fe_3GaTe_2 at an angle (without substrate rotation) to achieve asymmetric edge coverage can result in symmetry breaking in the SOT system to allow field-free magnetization switching of the PMA magnet. These studies collectively establish a robust foundation for the development of vdW magnet-based spintronic devices for room-temperature operation. The consistently low switching current density, high spin–orbit torque efficiency, and room-temperature operability of Fe_3GaTe_2/Pt system, which demonstrated across multiple studies, underscore its potential as a key component in the next generation of spintronic devices.

One challenge to the technological implementation of heavy metal or TI-based SOT devices is the requirement for an in-plane magnetic field, aligned with the current, to enable switching of magnets with PMA. This necessity arises from the mirror symmetry inherent in conventional heavy metals and TIs, which prevents the generation of an out-of-plane anti-damping torque. The constraint can be overcome by selecting spin-Hall materials that exhibit a broken mirror symmetry. Notably, vdW Weyl semimetals like the transition-metal dichalcogenides WTe_2[21,57,58] and monoclinic (β or 1 T') $MoTe_2$[59,60] exhibit out-of-plane anti-damping torque components due to their broken mirror symmetry. This effect was recently leveraged to achieve the field-free deterministic switching of Fe_3GaTe_2 above room temperature. Herein, Kajale et al. utilized the heterostructure of Fe_3GaTe_2 and T_d-WTe_2, leveraging the unconventional out-of-plane anti-damping torque generated by the spin-Hall effect in WTe_2[33] [Fig. 3(c, d)]. Field-free, deterministic switching of Fe_3GaTe_2 magnetization could be achieved using a low-current density of 2.23×10^6 A cm^{-2} at room temperatures. Robust, non-volatile switching of the PMA magnetization could be observed up to 320 K without any external magnetic fields, when current was applied along the low-symmetry a-axis of the material, as shown in Fig. 3(e). However, when current was applied along the high-symmetry b-axis, field-free deterministic switching was not observed. Instead, the ferromagnet was found to simply demagnetize at high current levels. These contrasting observations depending on the direction of applied current clearly elucidate the role of symmetry breaking in enabling field-free switching in such an all-vdW spin–orbit torque system.

Along similar lines, Zhang et al. have recently reported a study on field-free switching in a $TaIrTe_4$/ Fe_3GaTe_2 heterostructure.[61] $TaIrTe_4$ has a crystal structure similar to T_d-WTe_2, wherein the W–W chain is replaced with alternating Ta–Ta and Ir–Ir units. Consequently, an out-of-plane anti-damping-like torque was predicted and verified for this material in recent studies. The $TaIrTe_4$/Fe_3GaTe_2 heterostructure achieves magnetization switching at a current density of 2.56×10^6 A cm^{-2} at room temperature (300 K). The spin–orbit torque efficiency of the out-of-plane anti-damping torque has been estimated at 0.37 using hysteresis loop shift measurements. The switching is robust, maintaining stability against external magnetic fields up to 252 mT, demonstrating the potential for efficient and stable SOT-based devices using vdW materials.

Another noteworthy development has been the field-free switching of Fe_3GeTe_2 using in-plane exchange bias.[62] CrSBr, a semiconducting vdW antiferromagnet with Neel temperature of 132 K, exhibits an in-plane easy axis anisotropy. When sufficiently thick (> 30 nm) CrSBr was coupled with Fe_3GeTe_2, an in-plane exchange bias was induced in the ferromagnet resulting in a steady-state magnetization tilted away from the out-of-plane direction. The resulting lateral symmetry breaking could be leveraged to achieve field-free switching using Pt as the spin-Hall layer in a Pt/ Fe_3GeTe_2/ CrSBr system. While these results were limited to low temperatures, limited by the T_c of Fe_3GeTe_2 and T_N of CrSBr, the general approach holds promise for all-vdW spintronic systems. In addition, we note that other sources of SOT may significantly influence magnetization switching, thereby enhancing switching efficiency. For example, further investigation into complex magnetic vdW multilayers could elucidate the role of SOTs generated by interfacial spin currents or the spin anomalous Hall effect.

A summary of all previous reports of spin–orbit torque switching in vdW ferromagnets is presented in Table I. In addition, Fig. 4 provides a comparison of various vdW ferromagnet-based SOT systems and representative bulk SOT systems in the temperature and switching current density space. The advancements captured here have established the potential of vdW materials in developing scalable, energy-efficient spintronic devices, paving the way for their integration into commercial applications. By leveraging the unique properties of vdW materials, such as scalability to monolayer thicknesses, low-current field-free switching, and minimal intermixing with tunnel barriers, the next generation of spintronic devices promises significant breakthroughs in energy-efficient computing technologies.

Table I. Summary of experimental reports on current-controlled switching of vdW ferromagnets (FM).

vdW ferromagnet	SOC material	FM metallicity, anisotropy	Fabrication method (FM, SOC layer)	Threshold switching current density (MA/cm^2)	Temperature (K)	Field-assisted/ field-free	SOT efficiency (ξ_{DL})	ξ_{DL} characterization method	References
Fe_3GeTe_2	Pt	Metallic, OOP	Exfoliation, sputtering	27	180	Field-assisted	0.14	SHH	Alghamdi et al. [51]
Fe_3GeTe_2	Pt	Metallic, OOP	Exfoliation, sputtering	9.25	130	Field-assisted	–	–	Wang et al. [52]
Fe_3GeTe_2	$(Bi,Sb)_2Te_3$	Metallic, OOP	MBE, MBE	1.7	180	Field-assisted	–	–	Fujimura et al. [53]
Fe_3GeTe_2	WTe_2	Metallic, OOP	Exfoliation, exfoliation	6.6	200	Field-free	–	–	Kao et al. [63]
Fe_3GeTe_2	WTe_2	Metallic, OOP	Exfoliation, exfoliation	3.90	150	Field-free	4.6	Hysteresis loop shift	Shin et al. [64]
Fe_3GeTe_2	WTe_2	Metallic, OOP	Exfoliation, exfoliation	5.90	120	Field-free	–	–	Wang et al. [65]
$Cr_2Ge_2Te_6$	Ta	Insulating, OOP	Exfoliation, sputtering	0.5	80	Field-assisted	–	–	Ostwal et al. [66]
$Cr_2Ge_2Te_6$	Pt	Insulating, OOP	Exfoliation, sputtering	0.15	–	Field-assisted	0.25	SHH	Gupta et al. [67]
1 T-$CrTe_2$	$ZrTe_2$	Metallic, IP	MBE, MBE	18	50	Field-assisted	0.014	ST-FMR	Ou et al. [68]
Fe_3GaTe_2	Pt	Metallic, OOP	Exfoliation, sputtering	1.69	300	Field-assisted	0.093	SHH	Kajale et al. [32]
Fe_3GaTe_2	Pt	Metallic, OOP	Exfoliation, sputtering	13	300	Field-assisted	0.28	SHH	Li et al. [55]
Fe_3GaTe_2	Pt	Metallic, OOP	Exfoliation, sputtering	4.8	300	Field-assisted	–	–	Yun et al. [56]
Fe_3GaTe_2	WTe_2	Metallic, OOP	Exfoliation, exfoliation	2.23	320	Field-free	–	–	Kajale et al. [33]
Fe_3GaTe_2	$TaIrTe_4$	Metallic, OOP	Exfoliation, exfoliation	2.56E+06	300	Field-free	0.37	Hysteresis loop shift	Zhang et al. [61]

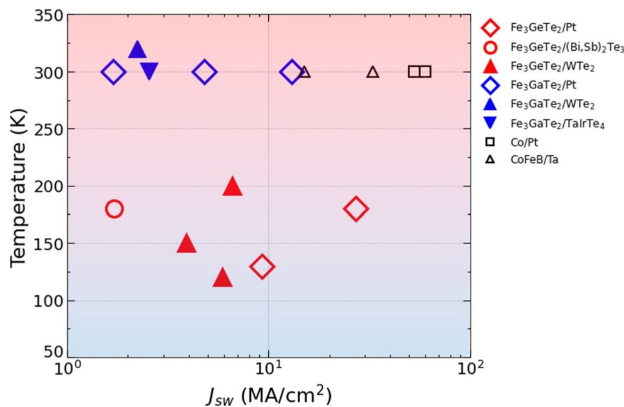

Figure. 4. Comparison of switching current density of metallic vdW ferromagnets with PMA, and representative bulk ferromagnets.[14,69–71] Hollow symbols and solid symbols represent field-assisted and field-free switching systems, respectively.

Future trends in vdW magnets-based spintronics

Wafer-scale growth

Developing protocols for wafer-scale growth of vdW magnetic materials is critical to their adoption in commercial spintronic devices. Wafer-scale growth techniques like molecular beam epitaxy (MBE) and chemical vapor deposition (CVD) can allow precise control of the vdW film thickness, composition, and magnetic anisotropy to open exciting prospects for developing advanced spintronic devices. However, challenges remain in achieving uniform, single-crystalline growth over large areas while maintaining the desired material properties.

Key issues include optimizing nucleation and growth conditions, minimizing defects and strain, identifying suitable substrates, and developing scalable precursors for metal-organic CVD.[72,73] The seamless merging of flakes to form large-area continuous films with well-controlled layer thickness and lattice orientation is still a significant challenge. In addition, understanding and controlling complex growth mechanisms, such as precursor sublimation, diffusion, nucleation, and

layer-by-layer growth, are crucial for improving repeatability and material quality. The stability of air-sensitive vdW magnets during transfer and processing is another concern, as many of these materials degrade in ambient conditions, hindering practical applications.

Despite these challenges, the progress in wafer-scale growth techniques has been promising. For instance, wafer-scale single-crystalline Fe_4GeTe_2 grown by MBE has shown strong magnetism with a T_c over 500 K, and its magnetic anisotropy can be flexibly controlled by tuning the Fe composition.[74] The epitaxial growth of single-crystalline $CrTe_2$ thin films on 2-inch sapphire substrates has demonstrated precise control of sample thickness and homogeneous surface morphology, which is essential for reliable magnetic memory applications.[75] Future research directions should focus on developing synthesis methods for large-scale and air-stable 2D magnetic crystals with high transition temperatures, as well as related vdW magnetic heterostructures.

Materials design

The vdW magnetic materials typically exhibit low T_c, which limit their practical application. This low T_C can compromise the stability of their magnetic properties during the integration process. In addition, their operational stability may be affected when high current density is injected for SOT generation. Fe_3GaTe_2 is fast emerging as a quintessential vdW ferromagnetic candidate for spintronics due to its high T_c and PMA. However, most studies related to its magnetic properties, current-based control, and incorporation into spintronic devices are limited to thick, exfoliated flakes. This raises concerns about its efficacy in the 2D limit where dimensionality effects are known to significantly decrease the T_c of magnetic materials. In fact, a recent study has reported a T_c of 240 K in an exfoliated monolayer of Fe_3GaTe_2, which although highest among all previous 2D magnets, is still well below the room temperature.[76] Certain approaches to overcoming this issue can be proposed upon examining other advances in the field. For example, attempting to increase the Fe content in the material, to achieve stoichiometries like Fe_4GaTe_2 and Fe_5GaTe_2 could be interesting. This trajectory has already been found to be fruitful in the closely related Fe_3GeTe_2, where the ferromagnetic T_C of the materials increased from ~210 K in Fe_3GeTe_2 to ~280 K–300 K in Fe_4GeTe_2[77] and Fe_5GeTe_2.[78] Another prospective path would be its epitaxial growth in conjunction with a suitable epilayer, like Bi_2Te_3. Growth of Fe_3GeTe_2 on sapphire substrates using MBE, with a Bi_2Te_3 epilayer, was found to raise the T_c of Fe_3GeTe_2 above room temperature.[79] Interestingly, it was reported that the T_C increases on reducing Fe_3GeTe_2 thicknesses, in contrast to what is expected from dimensionality effect. Similar improvement of T_c has also been reported in the case of Fe_5GeTe_2/Bi_2Te_3 epitaxial films,[80] adding more credibility to this approach for pushing the T_c of Fe_3GaTe_2 further.

Moreover, vdW magnetic materials are highly sensitive to ambient conditions, particularly to oxygen (O_2) and water (H_2O) molecules.[81,82] This exposure can lead to changes in their magnetic properties, a phenomenon that is often more pronounced in thinner vdW layers. The magnetic properties can vary significantly even in materials with the same stoichiometry and thickness, depending on the specific treatment and handling. This variability greatly impacts the robustness of magnetic switching. To mitigate this instability, encapsulation with materials such as hexagonal boron nitride (h-BN) is widely employed, as it prevents oxidation and provides high thermal stability before the materials are exposed to ambient conditions. Notably, Fe_3GaTe_2 has been reported to exhibit self-protection after an initial reaction with air, maintaining stable magnetic properties. However, this self-passivation requires relatively thick layers, such as 8 monolayers.

The material space for vdW magnetic insulators remains limited and confined to very low temperatures. In addition, the high sensitivity of these materials to ambient conditions poses challenges for stability during both the integration process and device operation. Focused efforts at realizing non-metallic vdW magnetic materials with high T_c can launch vdW magnets into magnonic devices. Similarly, there also exists a significant gap in the discovery of room-temperature 2D antiferromagnets and their spin manipulation properties. Antiferromagnets offer significant advantages, including the absence of stray fields and the potential for ultrafast spin dynamics, which can facilitate unprecedented performance in spintronics devices.

When designing new materials, it is worth noting that a significant advantage of the vast library of vdW magnetic materials experimentally realized to date is their composition, which predominantly includes transition metals and p-block elements while being largely free of rare-earth elements. This composition not only simplifies the synthesis of these materials but also aligns with sustainable practices. The absence of rare-earth elements, which are both expensive and environmentally destructive to mine, is a key feature that enhances the commercial viability of vdW magnets for spintronics applications.

Current-based control of magnetic anisotropy

An intriguing property of vdW magnetic materials like Fe_3GeTe_2 and Fe_3GaTe_2 is the possibility of tuning their magneto-crystalline anisotropy using in-plane currents. These hexagonal crystals belonging to the point group $\overline{6}$ m2 generate an intrinsic spin–orbit torque like magnetic field of the form.[83]

$$H_{SOT} = H_{SOT}\left\{\left(m_xJ_x - m_yJ_y\right)\hat{x} - \left(m_yJ_x + m_xJ_y\right)\hat{y}\right\},$$

where $J = J_x\hat{x} + J_y\hat{y}$ is the in-plane current density. Interestingly, there exists a free energy functional $f_{SOT}(m)$ such that $H_{SOT} = -M_s^{-1}\delta f_{SOT}(m)/\delta m$ and is given by

$$f_{SOT}(m) = M_sH_{SOT}\left\{J_ym_xm_y - \frac{1}{2}J_x(m_x^2 - m_y^2)\right\},$$

which when added to the effective free energy density of the ferromagnet, appears as an in-plane magneto-crystalline anisotropy term. Thus, applying an in-plane current to Fe_3GeTe_2 and

Fe_3GaTe_2 can effectively reduce their out-of-plane magnetic anisotropy dynamically,[83] creating a lower energy barrier for spin–orbit torque switching similar to what has been observed in voltage-based control of magnetic anisotropy (VCMA)-assisted SOT switching.[84] This effect also lends itself as a plausible explanation for the low switching current densities observed in SOT systems comprising these materials. Given that the applied current effectively reduces the out-of-plane anisotropy of the ferromagnet, it can reduce the magnon gap in the 2D Ising limit, in turn reducing the T_c in few-layer Fe_3GeTe_2 and Fe_3GaTe_2. Thus, a trade-off between current-assisted lowering of SOT switching barrier and the T_c may arise when using these materials.

Evidence of current-based control of magnetic anisotropy (CCMA) in these materials has also been reported in a series of recent experimental studies, by the observation of current-dependent coercivity tuning.[85–88] Zhang et al. have reported a 100% drop in the coercivity of Fe_3GeTe_2 nanosheets in response to an in-plane current density of 3×10^6 A cm^{-2} at 2 K.[85] Similar effect was reported by Yan et al. in Fe_3GaTe_2 at room temperature, where ~ 100% drop is coercivity could be achieved using a current density of 1.4×10^6 A cm^{-2}, as shown in Fig. 5(a, b). Thus, the CCMA effect in vdW magnets adds a new control mechanism for advanced spintronic devices.

Voltage or strain-based control of magnetic anisotropy

The switching current density of technologically relevant PMA ferromagnets is strongly correlated with their (out-of-plane) uniaxial anisotropy energy (K_U). Lowering K_U can help lower switching current density and in turn reduce energy consumption. However, choosing a ferromagnet with intrinsically low K_U is detrimental to the thermal stability of the magnetic devices. Thus, an optimal approach is to transiently lower the K_U of the ferromagnet while switching is being performed and restore the high K_U value once switching is completed. Such transient modulation of ferromagnetic K_U can be achieved by subjecting the ferromagnet to an electric field (voltage) or strain.[90]

In the case of VCMA, electric field applied across a ferromagnet-oxide interface can alter the interface electronic structure, including the redistribution of electron occupancies of the out-of-plane d_{z^2} and the in-plane $d_{x^2-y^2}, d_{xy}$ orbitals.[91,92] This affects the spin–orbit coupling in the ferromagnet and allows modulation of the magneto-crystalline anisotropy. Similarly, lattice distortions from straining a ferromagnet can alter its electronics structure, spin–orbit coupling, and hence, magneto-crystalline anisotropy. The ferromagnet can be strained electrically by coupling it with a piezoelectric, to create a magnetoelectric composite.[93,94] It is evident that both voltage and strain-based modulation of magnetic anisotropy are interface-driven phenomena and most effective when the ferromagnet thickness is only a few nanometers thick. Thus, vdW magnetic materials, which retain their structure and magnetic properties down to monolayer thicknesses, are seen as promising candidates for leveraging voltage and strain to achieve energy-efficient spintronic devices. While the direct integration of VCMA or strain-based tuning in vdW magnet SOT switching systems is still missing, several experimental efforts have revealed the effects of voltage and strain on the properties of vdW magnets.

Gate-tunable magnetic anisotropy in Fe_3GeTe_2 was first demonstrated through electrolyte gating experiments, which electrically controlled the magnetic properties by tuning the density of states (DOS).[95] These experiments revealed that ferromagnetism in thin Fe_3GeTe_2 could be drastically modulated, elevating the ferromagnetic transition temperature to room temperature and significantly altering the coercivity. Furthermore, the transition from an out-of-plane to an in-plane magnetic easy axis was achieved in Fe_5GeTe_2 by gating, which modulated the itinerant electron screening effect, effectively shifting the anisotropy constant from positive to negative,[89] as shown in Fig. 5(c–e). While electrolyte gating has been effective in inducing extreme doping in van der Waals ferromagnets, it presents limitations compared to the solid-gate approach. Nevertheless, these findings open up exciting possibilities for *in situ* voltage-controlled magnetoelectronics in vdW ferromagnets, paving the way for advanced spintronic devices.

Similarly, strain can profoundly influence the magnetic ordering in vdW systems. Li et al. showed that applying hydrostatic pressure to CrI_3 can induce a phase transition from interlayer antiferromagnetism to ferromagnetism.[96] Xu et al. demonstrated through first-principles calculations that applying ferroelastic strain to chromium sulfide halides (CrSX, where X = Cl, Br, I) monolayers can reversibly induce a 90° in-plane rotation of the magnetic easy axis.[97]

Magneto tunnel junction in all-vdW materials

MTJ, consisting of two ferromagnet layers separated by a thin-insulating barrier, is a fundamental building block for spintronic non-volatile memory devices.[1,2,98] MTJs are of great interest due to their high thermal stability and low critical current required for current-induced magnetization switching. Large tunnel magnetoresistance (TMR), which depends on the relative magnetization orientation of the free and fixed ferromagnet layers, is essential as it determines the on/off ratio in MTJs. TMR is highly sensitive to interface quality, including grain boundaries and lattice mismatch at the ferromagnet/tunneling barrier interface.[31,99–101] Utilizing atomically thin vdW materials in MTJs is expected to achieve giant TMR, as vdW materials alleviate the stringent lattice matching requirements associated with epitaxial growth and enable high-quality integration of dissimilar materials with atomically sharp interfaces.

Recent studies have demonstrated the feasibility of MTJs composed entirely of vdW materials.[102–106] For example, MTJs using an insulating CrI_3 thin layer as a tunnel barrier sandwiched between graphite contacts have shown remarkable TMR values ranging from 530% to 19,000%, depending on the number of CrI_3 layers.[102] The TMR of

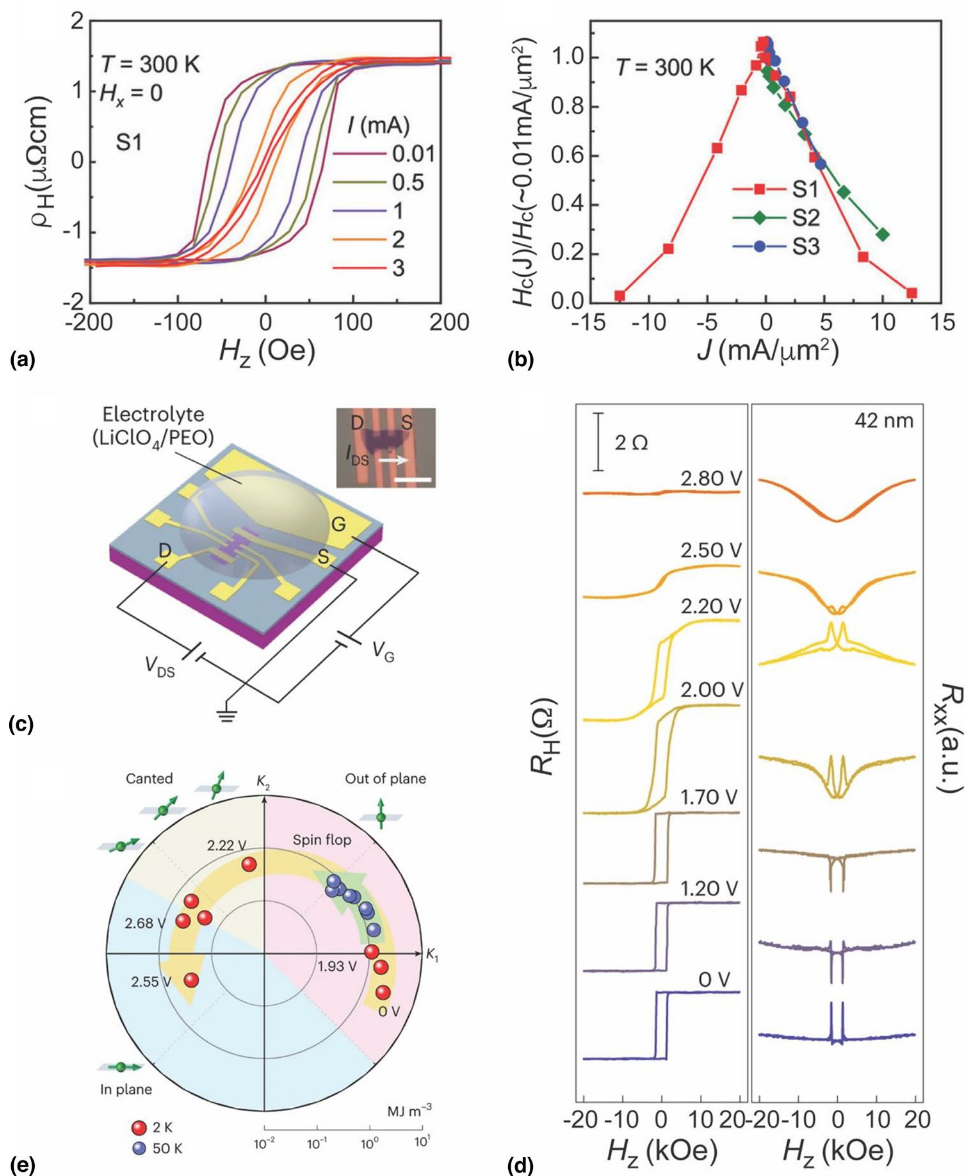

Figure. 5. (a) Anomalous Hall resistance recorded for Fe_3GaTe_2 at varying current level at 300 K. (b) Variation of coercivity of the Fe_3GaTe_2 nanosheets with respect to the applied current density. Reproduced with permission from Copyright © 2024, Yan et al. [87]. (c) Schematic illustration and optical image of the Hall-bar geometry for electrolyte gating. Here, gating electrolyte is a solution of $LiClO_4$ and PEO. The electrodes with D, S, and G represent the drain, source, and gate, respectively. (d) R_H and R_{xx} as a function of V_G at 2K. (e) Polar chart of gate-dependent anisotropy constant K_1 and K_2 of the Fe_5GeTe_2 flake with a thickness of 23 nm at 2 K (red circles) and 50 K (blue circles). Different colored areas represent three different spin orientation states: in-plane (light blue), out-of-plane (light pink), and canted (light yellow) spin orientations. Copyright © 2023, Tang et al. [89].

19,000% is significantly higher than that reported in conventional MTJs,[107] indicating the potential of all-vdW MTJ devices, despite the current operation temperature being at 2 K. For high-temperature MTJ operation, metallic Fe_3GeTe_2 and Fe_3GaTe_2 -based MTJs have been widely investigated.[103–106] Notably, TMR values up to 192% at 10 K in $Fe_3GeTe_2/GaSe/Fe_3GeTe_2$ MTJs and 85% in $Fe_3GeTe_2/WSe_2/Fe_3GeTe_2$ MTJs at room temperature have been observed.[106] In $Fe_3GaTe_2/MoS_2/Fe_3GaTe_2$ MTJs and $Fe_3GaTe_2/MoSe_2/Fe_3GaTe_2$ MTJs, TMR of 0.31% and 3% has been reported at room temperature.[108,109] With WSe_2 and WS_2 tunnel barrier, TMR shows 85% and 11% at room temperature.[110,111] Although the current state of vdW-based MTJs requires improvements, such as achieving high TMR at room temperature and wafer-scale growth for device integration, the fundamental properties of vdW ferromagnet

materials significantly expand material design opportunities for future non-volatile memory devices.

Conclusion

In this paper, we presented a comprehensive review of the current research on current-based control of vdW magnetic materials and their potential in developing energy-efficient spintronic devices. We discussed the rapid advancements in spintronics and emphasized the importance of vdW magnetic materials, particularly their unique-layered structures, which allow them to retain magnetic properties down to the monolayer limit. The discovery of intrinsic ferromagnetism with a high Curie temperature and large perpendicular magnetic anisotropy makes these materials strong contenders for future spintronic technologies. Their scalability, high interface quality, and efficient spin transfer offer significant advantages for miniaturized, energy-efficient, and high-density spintronic applications. With continued progress in overcoming current challenges, vdW magnets hold great promise for seamless integration into next-generation devices.

Author contributions

J.R. and S.K. equally contributed to literature search, conceptualization, visualization, and writing the manuscript. D.S. contributed to conceptualization, editing, revision, and supervision.

Funding

Open Access funding provided by the MIT Libraries. This work and finding are provided by Sarkar's MIT startup funding.

Data availability

Not applicable.

Declarations

Conflict of interest

The authors declare no conflict of interest.

Open Access

This article is licensed under a Creative Commons Attribution 4.0 International License, which permits use, sharing, adaptation, distribution and reproduction in any medium or format, as long as you give appropriate credit to the original author(s) and the source, provide a link to the Creative Commons licence, and indicate if changes were made. The images or other third party material in this article are included in the article's Creative Commons licence, unless indicated otherwise in a credit line to the material. If material is not included in the article's Creative Commons licence and your intended use is not permitted by statutory regulation or exceeds the permitted use, you will need to obtain permission directly from the copyright holder. To view a copy of this licence, visit http://creativecommons.org/licenses/by/4.0/.

References

1. I. Žutić, J. Fabian, S. Das Sarma, Spintronics: fundamentals and applications. Rev. Mod. Phys. **76**, 323–410 (2004)
2. S.A. Wolf, D.D. Awschalom, R.A. Buhrman, J.M. Daughton, S. von Molnár, M.L. Roukes, A.Y. Chtchelkanova, D.M. Treger, Spintronics: a spin-based electronics vision for the future. Science (1979) **294**, 1488–1495 (2001)
3. C. Gong, X. Zhang, Two-dimensional magnetic crystals and emergent heterostructure devices. Science **363**, 6428 (2019)
4. M. Gibertini, M. Koperski, A.F. Morpurgo, K.S. Novoselov, Magnetic 2D materials and heterostructures. Nat. Nanotechnol. **14**, 408–419 (2019)
5. S.N. Kajale, J. Hanna, K. Jang, D. Sarkar, Two-dimensional magnetic materials for spintronic applications. Nano Res. **17**, 743–762 (2024)
6. C. Gong, L. Li, Z. Li, H. Ji, A. Stern, Y. Xia, T. Cao, W. Bao, C. Wang, Y. Wang, Z.Q. Qiu, R.J. Cava, S.G. Louie, J. Xia, X. Zhang, Discovery of intrinsic ferromagnetism in two-dimensional van der Waals crystals. Nature **546**, 265–269 (2017)
7. B. Huang, G. Clark, E. Navarro-Moratalla, D.R. Klein, R. Cheng, K.L. Seyler, D. Zhong, E. Schmidgall, M.A. McGuire, D.H. Cobden, W. Yao, D. Xiao, P. Jarillo-Herrero, X. Xu, Layer-dependent ferromagnetism in a van der Waals crystal down to the monolayer limit. Nature **546**, 270–273 (2017)
8. Z. Fei, B. Huang, P. Malinowski, W. Wang, T. Song, J. Sanchez, W. Yao, D. Xiao, X. Zhu, A.F. May, W. Wu, D.H. Cobden, J.H. Chu, X. Xu, Two-dimensional itinerant ferromagnetism in atomically thin Fe3GeTe2. Nat. Mater. **17**, 778–782 (2018)
9. G. Zhang, F. Guo, H. Wu, X. Wen, L. Yang, W. Jin, W. Zhang, H. Chang, Above-room-temperature strong intrinsic ferromagnetism in 2D van der Waals Fe_3GaTe_2 with large perpendicular magnetic anisotropy. Nat. Commun. **13**, 1–8 (2022)
10. L. Berger, Emission of spin waves by a magnetic multilayer traversed by a current. Phys. Rev. B **54**, 9353–9358 (1996)
11. J.C. Slonczewski, Current-driven excitation of magnetic multilayers. J. Magn. Magn. Mater. **159**, L1–L7 (1996)
12. A. Manchon, J. Železný, I.M. Miron, T. Jungwirth, J. Sinova, A. Thiaville, K. Garello, P. Gambardella, Current-induced spin-orbit torques in ferromagnetic and antiferromagnetic systems. Rev. Mod. Phys. **91**, 35004 (2019)
13. I.M. Miron, K. Garello, G. Gaudin, P.-J. Zermatten, M.V. Costache, S. Auffret, S. Bandiera, B. Rodmacq, A. Schuhl, P. Gambardella, Perpendicular switching of a single ferromagnetic layer induced by in-plane current injection. Nature **476**, 189–193 (2011)
14. L. Liu, C.-F. Pai, Y. Li, H.W. Tseng, D.C. Ralph, R.A. Buhrman, Spin-torque switching with the giant spin hall effect of tantalum. Science **1979**(336), 555–558 (2012)
15. J. Kim, J. Sinha, M. Hayashi, M. Yamanouchi, S. Fukami, T. Suzuki, S. Mitani, H. Ohno, Layer thickness dependence of the current-induced effective field vector in TalCoFeBlMgO. Nat. Mater. **12**, 240–245 (2013)
16. K. Garello, I.M. Miron, C.O. Avci, F. Freimuth, Y. Mokrousov, S. Blügel, S. Auffret, O. Boulle, G. Gaudin, P. Gambardella, Symmetry and magnitude of spin-orbit torques in ferromagnetic heterostructures. Nat. Nanotechnol. **8**, 587–593 (2013)
17. Y.K. Kato, R.C. Myers, A.C. Gossard, D.D. Awschalom, Observation of the spin hall effect in semiconductors. Science **1979**(306), 1910–1913 (2004)
18. V.M. Edelstein, Spin polarization of conduction electrons induced by electric current in two-dimensional asymmetric electron systems. Solid State Commun. **73**, 233–235 (1990)
19. M. Baumgartner, K. Garello, J. Mendil, C.O. Avci, E. Grimaldi, C. Murer, J. Feng, M. Gabureac, C. Stamm, Y. Acremann, S. Finizio, S. Wintz, J. Raabe, P. Gambardella, Spatially and time-resolved magnetization dynamics driven by spin–orbit torques. Nat. Nanotechnol. **12**, 980–986 (2017)
20. G. Choi, J. Ryu, R. Thompson, J.-G. Choi, J. Jeong, S. Lee, M.-G. Kang, M. Kohda, J. Nitta, B.-G. Park, Thickness dependence of spin–orbit torques in Pt/Co structures on epitaxial substrates. APL Mater. **10**, 011105 (2022)

21. D. MacNeill, G.M. Stiehl, M.H.D. Guimaraes, R.A. Buhrman, J. Park, D.C. Ralph, Control of spin–orbit torques through crystal symmetry in WTe2/ferromagnet bilayers. Nat. Phys. **13**, 300–305 (2017)
22. P. Li, W. Wu, Y. Wen, C. Zhang, J. Zhang, S. Zhang, Z. Yu, S.A. Yang, A. Manchon, X. Zhang, Spin-momentum locking and spin-orbit torques in magnetic nano-heterojunctions composed of Weyl semimetal WTe2. Nat. Commun. **9**, 3990 (2018)
23. X. Chen, S. Shi, G. Shi, X. Fan, C. Song, X. Zhou, H. Bai, L. Liao, Y. Zhou, H. Zhang, A. Li, Y. Chen, X. Han, S. Jiang, Z. Zhu, H. Wu, X. Wang, D. Xue, H. Yang, F. Pan, Observation of the antiferromagnetic spin Hall effect. Nat. Mater. **20**, 800–804 (2021)
24. R. González-Hernández, L. Šmejkal, K. Výborný, Y. Yahagi, J. Sinova, T. Jungwirth, J. Železný, Efficient electrical spin splitter based on nonrelativistic collinear antiferromagnetism. Phys. Rev. Lett. **126**, 127701 (2021)
25. M. Kimata, H. Chen, K. Kondou, S. Sugimoto, P.K. Muduli, M. Ikhlas, Y. Omori, T. Tomita, H. Allan, S.N. MacDonald, Y. Otani, Magnetic and magnetic inverse spin Hall effects in a non-collinear antiferromagnet. Nature **565**, 627–630 (2019)
26. Y. Liu, Y. Liu, M. Chen, S. Srivastava, P. He, K.L. Teo, T. Phung, S.-H. Yang, H. Yang, Current-induced out-of-plane spin accumulation on the (001) surface of the IrMn3 antiferromagnet. Phys. Rev. Appl. **12**, 64046 (2019)
27. H. Bai, L. Han, X.Y. Feng, Y.J. Zhou, R.X. Su, Q. Wang, L.Y. Liao, W.X. Zhu, X.Z. Chen, F. Pan, X.L. Fan, C. Song, Observation of spin splitting torque in a collinear antiferromagnet RuO_2. Phys. Rev. Lett. **128**, 197202 (2022)
28. T. Nan, C.X. Quintela, J. Irwin, G. Gurung, D.F. Shao, J. Gibbons, N. Campbell, K. Song, S.-Y. Choi, L. Guo, R.D. Johnson, P. Manuel, R.V. Chopdekar, I. Hallsteinsen, T. Tybell, P.J. Ryan, J.-W. Kim, Y. Choi, P.G. Radaelli, D.C. Ralph, E.Y. Tsymbal, M.S. Rzchowski, C.B. Eom, Controlling spin current polarization through non-collinear antiferromagnetism. Nat. Commun. **11**, 4671 (2020)
29. S. Mangin, D. Ravelosona, J.A. Katine, M.J. Carey, B.D. Terris, E.E. Fullerton, Current-induced magnetization reversal in nanopillars with perpendicular anisotropy. Nat. Mater. **5**, 210–215 (2006)
30. H.X. Yang, M. Chshiev, B. Dieny, J.H. Lee, A. Manchon, K.H. Shin, First-principles investigation of the very large perpendicular magnetic anisotropy at FelMgO and ColMgO interfaces. Phys. Rev. B **84**, 54401 (2011)
31. C.H. Back, Ch. Würsch, A. Vaterlaus, U. Ramsperger, U. Maier, D. Pescia, Experimental confirmation of universality for a phase transition in two dimensions. Nature **378**, 597–600 (1995)
32. S.N. Kajale, T. Nguyen, C.A. Chao, D.C. Bono, A. Boonkird, M. Li, D. Sarkar, Current-induced switching of a van der Waals ferromagnet at room temperature. Nat. Commun. **15**, 1485 (2024)
33. S.N. Kajale, T. Nguyen, N.T. Hung, M. Li, D. Sarkar, Field-free deterministic switching of all–van der Waals spin-orbit torque system above room temperature. Sci. Adv. **10**, eadk8669 (2024)
34. S. Fukami, C. Zhang, S. DuttaGupta, A. Kurenkov, H. Ohno, Magnetization switching by spin–orbit torque in an antiferromagnet–ferromagnet bilayer system. Nat. Mater. **15**, 535–541 (2016)
35. Y.-W. Oh, S. Chris Baek, Y.M. Kim, H.Y. Lee, K.-D. Lee, C.-G. Yang, E.-S. Park, K.-S. Lee, K.-W. Kim, G. Go, J.-R. Jeong, B.-C. Min, H.-W. Lee, K.-J. Lee, B.-G. Park, Field-free switching of perpendicular magnetization through spin–orbit torque in antiferromagnet/ferromagnet/oxide structures. Nat. Nanotechnol. **11**, 878–884 (2016)
36. W.-Y. Kwak, J.-H. Kwon, P. Grünberg, S.H. Han, B.K. Cho, Current-induced magnetic switching with spin-orbit torque in an interlayer-coupled junction with a Ta spacer layer. Sci. Rep. **8**, 3826 (2018)
37. J. Wei, X. Wang, B. Cui, C. Guo, H. Xu, Y. Guang, Y. Wang, X. Luo, C. Wan, J. Feng, H. Wei, G. Yin, X. Han, G. Yu, Field-free spin-orbit torque switching in perpendicularly magnetized synthetic antiferromagnets. Adv. Funct. Mater. **32**, 2109455 (2022)
38. S.C. Baek, V.P. Amin, Y.-W. Oh, G. Go, S.-J. Lee, G.-H. Lee, K.-J. Kim, M.D. Stiles, B.-G. Park, K.-J. Lee, Spin currents and spin–orbit torques in ferromagnetic trilayers. Nat. Mater. **17**, 509–513 (2018)
39. Z. Zheng, Y. Zhang, V. Lopez-Dominguez, L. Sánchez-Tejerina, J. Shi, X. Feng, L. Chen, Z. Wang, Z. Zhang, K. Zhang, B. Hong, Y. Xu, Y. Zhang, M. Carpentieri, A. Fert, G. Finocchio, W. Zhao, P. Khalili Amiri, Field-free spin-orbit torque-induced switching of perpendicular magnetization in a ferrimagnetic layer with a vertical composition gradient. Nat. Commun. **12**, 4555 (2021)
40. J. Ryu, C.O. Avci, M. Song, M. Huang, R. Thompson, J. Yang, S. Ko, S. Karube, N. Tezuka, M. Kohda, K.-J. Kim, G.S.D. Beach, J. Nitta, Deterministic current-induced perpendicular switching in epitaxial Co/Pt layers without an external field. Adv. Funct. Mater. **33**, 2209693 (2023)
41. S. Iihama, T. Taniguchi, K. Yakushiji, A. Fukushima, Y. Shiota, S. Tsunegi, R. Hiramatsu, S. Yuasa, Y. Suzuki, H. Kubota, Spin-transfer torque induced by the spin anomalous Hall effect. Nat. Electron. **1**, 120–123 (2018)
42. J. Ryu, R. Thompson, J.Y. Park, S.-J. Kim, G. Choi, J. Kang, H.B. Jeong, M. Kohda, J.M. Yuk, J. Nitta, K.-J. Lee, B.-G. Park, Efficient spin-orbit torque in magnetic trilayers using all three polarizations of a spin current. Nat. Electron. **5**, 217–223 (2022)
43. G. Yu, P. Upadhyaya, Y. Fan, J.G. Alzate, W. Jiang, K.L. Wong, S. Takei, S.A. Bender, L.-T. Chang, Y. Jiang, M. Lang, J. Tang, Y. Wang, Y. Tserkovnyak, P.K. Amiri, K.L. Wang, Switching of perpendicular magnetization by spin-orbit torques in the absence of external magnetic fields. Nat. Nanotechnol. **9**, 548–554 (2014)
44. V. Krizakova, E. Grimaldi, K. Garello, G. Sala, S. Couet, G.S. Kar, P. Gambardella, Interplay of voltage control of magnetic anisotropy, spin-transfer torque, and heat in the spin-orbit-torque switching of three-terminal magnetic tunnel junctions. Phys. Rev. Appl. **15**, 54055 (2021)
45. C.O. Avci, K. Garello, C. Nistor, S. Godey, B. Ballesteros, A. Mugarza, A. Barla, M. Valvidares, E. Pellegrin, A. Ghosh, I.M. Miron, O. Boulle, S. Auffret, G. Gaudin, P. Gambardella, Fieldlike and antidamping spin-orbit torques in as-grown and annealed Ta/CoFeB/MgO layers. Phys. Rev. B **89**, 214419 (2014)
46. M. Dc, D.F. Shao, V.D.H. Hou, A. Vailionis, P. Quarterman, A. Habiboglu, M.B. Venuti, F. Xue, Y.L. Huang, C.M. Lee, M. Miura, Observation of anti-damping spin–orbit torques generated by in-plane and out-of-plane spin polarizations in MnPd3. Nat. Mater. **22**, 591–598 (2023)
47. Y. Zhang, H. Xu, K. Jia, G. Lan, Z. Huang, B. He, C. He, Q. Shao, Y. Wang, M. Zhao, T. Ma, J. Dong, C. Guo, C. Cheng, J. Feng, C. Wan, H. Wei, Y. Shi, G. Zhang, X. Han, G. Yu, Room temperature field-free switching of perpendicular magnetization through spin-orbit torque originating from low-symmetry type II Weyl semimetal. Sci. Adv. **9**, eadg9819 (2024)
48. Y. Liu, G. Shi, D. Kumar, T. Kim, S. Shi, D. Yang, J. Zhang, C. Zhang, F. Wang, S. Yang, Y. Pu, P. Yu, K. Cai, H. Yang, Field-free switching of perpendicular magnetization at room temperature using out-of-plane spins from TaIrTe4. Nat. Electron. **6**, 732–738 (2023)
49. X. Fan, J. Wu, Y. Chen, M.J. Jerry, H. Zhang, J.Q. Xiao, Observation of the nonlocal spin-orbital effective field. Nat. Commun. **4**, 1799 (2013)
50. Th. Gerrits, H.A.M. van den Berg, J. Hohlfeld, L. Bär, Th. Rasing, Ultrafast precessional magnetization reversal by picosecond magnetic field pulse shaping. Nature **418**, 509–512 (2002)
51. M. Alghamdi, M. Lohmann, J. Li, P.R. Jothi, Q. Shao, M. Aldosary, T. Su, B.P.T. Fokwa, J. Shi, Highly efficient spin-orbit torque and switching of layered ferromagnet Fe_3GeTe_2. Nano Lett. **19**, 4400–4405 (2019)
52. X. Wang, J. Tang, X. Xia, C. He, J. Zhang, Y. Liu, C. Wan, C. Fang, C. Guo, W. Yang, Y. Guang, X. Zhang, H. Xu, J. Wei, M. Liao, X. Lu, J. Feng, X. Li, Y. Peng, H. Wei, R. Yang, D. Shi, X. Zhang, Z. Han, Z. Zhang, G. Zhang, G. Yu, X. Han, Current-driven magnetization switching in a van der Waals ferromagnet Fe_3GeTe_2. Sci. Adv. **5**, eaaw8904 (2024)
53. R. Fujimura, R. Yoshimi, M. Mogi, A. Tsukazaki, M. Kawamura, K.S. Takahashi, M. Kawasaki, Y. Tokura, Current-induced magnetization switching at charge-transferred interface between topological insulator $(Bi, Sb)_2Te_3$ and van der Waals ferromagnet Fe_3GeTe_2. Appl. Phys. Lett. **119**, 032402 (2021)
54. A.M. Ruiz, D.L. Esteras, D. López-Alcalá, J.J. Baldoví, On the origin of the above-room-temperature magnetism in the 2D van der Waals Ferromagnet Fe_3GaTe_2. Nano Lett. (2024). https://doi.org/10.1021/acs.nanolett.4c01019
55. W. Li, W. Zhu, G. Zhang, H. Wu, S. Zhu, R. Li, E. Zhang, X. Zhang, Y. Deng, J. Zhang, L. Zhao, H. Chang, K. Wang, Room-temperature van der Waals ferromagnet switching by spin-orbit torques. Adv. Mater. **35**, 2303688 (2023)
56. C. Yun, H. Guo, Z. Lin, L. Peng, Z. Liang, M. Meng, B. Zhang, Z. Zhao, L. Wang, Y. Ma, Y. Liu, W. Li, S. Ning, Y. Hou, J. Yang, Z. Luo, Efficient current-induced spin torques and field-free magnetization switching in a room-temperature van der Waals magnet. Sci. Adv. **9**, eadj3955 (2024)

57. D. MacNeill, G.M. Stiehl, M.H.D. Guimarães, N.D. Reynolds, R.A. Buhrman, D.C. Ralph, Thickness dependence of spin-orbit torques generated by WTe_2. Phys. Rev. B **96**, 54450 (2017)
58. S. Shi, S. Liang, Z. Zhu, K. Cai, S.D. Pollard, Y. Wang, J. Wang, Q. Wang, P. He, J. Yu, G. Eda, G. Liang, H. Yang, All-electric magnetization switching and Dzyaloshinskii-Moriya interaction in WTe_2/ferromagnet heterostructures. Nat. Nanotechnol. **14**, 945–949 (2019)
59. S. Liang, S. Shi, C.-H. Hsu, K. Cai, Y. Wang, P. He, Y. Wu, V.M. Pereira, H. Yang, Spin-orbit torque magnetization switching in $MoTe_2$/permalloy heterostructures. Adv. Mater. **32**, 2002799 (2020)
60. G.M. Stiehl, R. Li, V. Gupta, I.E. Baggari, S. Jiang, H. Xie, L.F. Kourkoutis, K.F. Mak, J. Shan, R.A. Buhrman, D.C. Ralph, Layer-dependent spin-orbit torques generated by the centrosymmetric transition metal dichalcogenide β-MoTe2. Phys. Rev. B **100**, 184402 (2019)
61. Y. Zhang, X. Ren, R. Liu, Z. Chen, X. Wu, J. Pang, W. Wang, G. Lan, K. Watanabe, T. Taniguchi, Y. Shi, G. Yu, Q. Shao, Robust field-free switching using large unconventional spin-orbit torque in an all-Van der Waals heterostructure. Adv. Mater. (2024). https://doi.org/10.1002/adma.202406464
62. T.M.J. Cham, R.J. Dorrian, X.S. Zhang, A.H. Dismukes, D.G. Chica, A.F. May, X. Roy, D.A. Muller, D.C. Ralph, Y.K. Luo, Exchange bias between van der Waals materials: tilted magnetic states and field-free spin–orbit-torque switching. Adv. Mater. (2024). https://doi.org/10.1002/adma.202305739
63. I.-H. Kao, R. Muzzio, H. Zhang, M. Zhu, J. Gobbo, S. Yuan, D. Weber, R. Rao, J. Li, J.H. Edgar, J.E. Goldberger, J. Yan, D.G. Mandrus, J. Hwang, R. Cheng, J. Katoch, S. Singh, Deterministic switching of a perpendicularly polarized magnet using unconventional spin-orbit torques in WTe_2. Nat. Mater. **21**, 1029–1034 (2022)
64. I. Shin, W.J. Cho, E.S. An, S. Park, H.W. Jeong, S. Jang, W.J. Baek, S.Y. Park, D.H. Yang, J.H. Seo, G.Y. Kim, M.N. Ali, S.Y. Choi, H.W. Lee, J.S. Kim, S.D. Kim, G.H. Lee, Spin-orbit torque switching in an all-Van der Waals heterostructure. Adv. Mater. **34**, 1–7 (2022)
65. L. Wang, J. Xiong, B. Cheng, Y. Dai, F. Wang, C. Pan, T. Cao, X. Liu, P. Wang, M. Chen, S. Yan, Z. Liu, J. Xiao, X. Xu, Z. Wang, Y. Shi, S.W. Cheong, H. Zhang, S.J. Liang, F. Miao, Cascadable in-memory computing based on symmetric writing and readout. Sci. Adv. **8**, 1–11 (2022)
66. V. Ostwal, T. Shen, J. Appenzeller, Efficient spin-orbit torque switching of the semiconducting Van Der Waals ferromagnet $Cr_2Ge_2Te_6$. Adv. Mater. **32**, 1–7 (2020)
67. V. Gupta, T.M. Cham, G.M. Stiehl, A. Bose, J.A. Mittelstaedt, K. Kang, S. Jiang, K.F. Mak, J. Shan, R.A. Buhrman, D.C. Ralph, Manipulation of the van der Waals magnet $Cr_2Ge_2Te_6$ by spin-orbit torques. Nano Lett. **20**, 7482–7488 (2020)
68. Y. Ou, W. Yanez, R. Xiao, M. Stanley, S. Ghosh, B. Zheng, W. Jiang, Y.S. Huang, T. Pillsbury, A. Richardella, C. Liu, T. Low, V.H. Crespi, K.A. Mkhoyan, N. Samarth, $ZrTe_2$/$CrTe_2$: an epitaxial van der Waals platform for spintronics. Nat. Commun. **13**, 1–9 (2022)
69. J. Ryu, C.O. Avci, S. Karube, M. Kohda, G.S.D. Beach, J. Nitta, Crystal orientation dependence of spin-orbit torques in Co/Pt bilayers. Appl. Phys. Lett. **114**, 142402 (2019)
70. C. Zhang, S. Fukami, H. Sato, F. Matsukura, H. Ohno, Spin-orbit torque induced magnetization switching in nano-scale Ta/CoFeB/MgO. Appl. Phys. Lett. **107**, 012401 (2015)
71. K. Garello, C.O. Avci, I.M. Miron, M. Baumgartner, A. Ghosh, S. Auffret, O. Boulle, G. Gaudin, P. Gambardella, Ultrafast magnetization switching by spin-orbit torques. Appl. Phys. Lett. **105**, 212402 (2014)
72. X. Xu, T. Guo, H. Kim, M.K. Hota, R.S. Alsaadi, M. Lanza, X. Zhang, H.N. Alshareef, Growth of 2D materials at the wafer scale. Adv. Mater. **34**, 2108258 (2022)
73. A. Dimoulas, Perspectives for the growth of epitaxial 2D van der Waals layers with an emphasis on ferromagnetic metals for spintronics. Adv. Mater. Interfaces **9**, 2201469 (2022)
74. H. Wang, H. Lu, Z. Guo, A. Li, P. Wu, J. Li, W. Xie, Z. Sun, P. Li, H. Damas, A.M. Friedel, S. Migot, J. Ghanbaja, L. Moreau, Y. Fagot-Revurat, S. Petit-Watelot, T. Hauet, J. Robertson, S. Mangin, W. Zhao, T. Nie, Interfacial engineering of ferromagnetism in wafer-scale van der Waals Fe_4GeTe_2 far above room temperature. Nat. Commun. **14**, 2483 (2023)
75. S. Liu, X. Yuan, Y. Zou, Y. Sheng, C. Huang, E. Zhang, J. Ling, Y. Liu, W. Wang, C. Zhang, J. Zou, K. Wang, F. Xiu, Wafer-scale two-dimensional ferromagnetic Fe_3GeTe_2 thin films grown by molecular beam epitaxy. NPJ 2D Mater. Appl. **1**, 1–6 (2017)
76. M. Wang, B. Lei, K. Zhu, Y. Deng, M. Tian, Z. Xiang, T. Wu, X. Chen, Hard ferromagnetism in van der Waals Fe_3GaTe_2 nanoflake down to monolayer. NPJ 2D Mater. Appl. **8**, 22 (2024)
77. J. Seo, D.Y. Kim, E.S. An, K. Kim, G.-Y. Kim, S.-Y. Hwang, D.W. Kim, B.G. Jang, H. Kim, G. Eom, S.Y. Seo, R. Stania, M. Muntwiler, J. Lee, K. Watanabe, T. Taniguchi, Y.J. Jo, J. Lee, B.I. Min, M.H. Jo, H.W. Yeom, S.-Y. Choi, J.H. Shim, J.S. Kim, Nearly room temperature ferromagnetism in a magnetic metal-rich van der Waals metal. Sci. Adv. **6**, 18912 (2020)
78. A.F. May, D. Ovchinnikov, Q. Zheng, R. Hermann, S. Calder, B. Huang, Z. Fei, Y. Liu, X. Xu, M.A. McGuire, Ferromagnetism near room temperature in the cleavable van der Waals crystal Fe_5GeTe_2. ACS Nano **13**, 4436–4442 (2019)
79. H. Wang, Y. Liu, P. Wu, W. Hou, Y. Jiang, X. Li, C. Pandey, D. Chen, Q. Yang, H. Wang, D. Wei, N. Lei, W. Kang, L. Wen, T. Nie, W. Zhao, K.L. Wang, Above room-temperature ferromagnetism in wafer-scale two-dimensional van der Waals Fe_3GeTe_2 tailored by a topological insulator. ACS Nano **14**, 10045–10053 (2020)
80. E. Georgopoulou-Kotsaki, P. Pappas, A. Lintzeris, P. Tsipas, S. Fragkos, A. Markou, C. Felser, E. Longo, M. Fanciulli, R. Mantovan, F. Mahfouzi, N. Kioussis, A. Dimoulas, Significant enhancement of ferromagnetism above room temperature in epitaxial 2D van der Waals ferromagnet Fe_5–δ$GeTe_2$/Bi_2Te_3 heterostructures. Nanoscale **15**, 2223–2233 (2023)
81. D. Shcherbakov, P. Stepanov, D. Weber, Y. Wang, J. Hu, Y. Zhu, K. Watanabe, T. Taniguchi, Z. Mao, W. Windl, J. Goldberger, M. Bockrath, C.N. Lau, Raman spectroscopy, photocatalytic degradation, and stabilization of atomically thin chromium tri-iodide. Nano Lett. **18**, 4214–4219 (2018)
82. Z. Tu, T. Xie, Y. Lee, J. Zhou, A.S. Admasu, Y. Gong, N. Valanoor, J. Cumings, S.-W. Cheong, I. Takeuchi, K. Cho, C. Gong, Ambient effect on the Curie temperatures and magnetic domains in metallic two-dimensional magnets. Mater. Appl. **5**, 62 (2021)
83. Ø. Johansen, V. Risinggård, A. Sudbø, J. Linder, A. Brataas, Current control of magnetism in two-dimensional Fe_3GeTe_2. Phys. Rev. Lett. **122**, 217203 (2019)
84. Y.C. Wu, K. Garello, W. Kim, M. Gupta, M. Perumkunnil, V. Kateel, S. Couet, R. Carpenter, S. Rao, S. Van Beek, K.K. Vudya Sethu, F. Yasin, D. Crotti, G.S. Kar, Voltage-gate-assisted spin-orbit-torque magnetic random-access memory for high-density and low-power embedded applications. Phys. Rev. Appl. **15**, 64015 (2021)
85. K. Zhang, S. Han, Y. Lee, M.J. Coak, J. Kim, I. Hwang, S. Son, J. Shin, M. Lim, D. Jo, K. Kim, D. Kim, H.-W. Lee, J.-G. Park, Gigantic current control of coercive field and magnetic memory based on nanometer-thin ferromagnetic van der Waals Fe_3GeTe_2. Adv. Mater. **33**, 2004110 (2021)
86. K. Zhang, Y. Lee, M.J. Coak, J. Kim, S. Son, I. Hwang, D.-S. Ko, Y. Oh, I. Jeon, D. Kim, C. Zeng, H.-W. Lee, J.-G. Park, Highly efficient nonvolatile magnetization switching and multi-level states by current in single Van der Waals topological ferromagnet Fe_3GeTe_2. Adv. Funct. Mater. **31**, 2105992 (2021)
87. S. Yan, S. Tian, Y. Fu, F. Meng, Z. Li, H. Lei, S. Wang, X. Zhang, Highly efficient room-temperature nonvolatile magnetic switching by current in Fe_3GaTe_2 thin flakes. Small **20**, 2311430 (2024)
88. G. Zhang, H. Wu, L. Yang, W. Jin, B. Xiao, W. Zhang, H. Chang, Room-temperature highly-tunable coercivity and highly-efficient multi-states magnetization switching by small current in single 2D ferromagnet Fe_3GaTe_2. ACS Mater. Lett. **6**, 482–488 (2024)
89. M. Tang, J. Huang, F. Qin, K. Zhai, T. Ideue, Z. Li, F. Meng, A. Nie, L. Wu, X. Bi, C. Zhang, L. Zhou, P. Chen, C. Qiu, P. Tang, H. Zhang, X. Wan, L. Wang, Z. Liu, Y. Tian, Y. Iwasa, H. Yuan, Continuous manipulation of magnetic anisotropy in a van der Waals ferromagnet via electrical gating. Nat Electron **6**, 28–36 (2023)
90. S. Yu, J. Tang, Y. Wang, F. Xu, X. Li, X. Wang, Recent advances in two-dimensional ferromagnetism: strain-, doping-, structural- and electric field-engineering toward spintronic applications. Sci. Technol. Adv. Mater. **23**(1), 140–160 (2022) https://doi.org/10.1080/14686996.2022.2030652
91. T. Nozaki, T. Yamamoto, S. Miwa, M. Tsujikawa, M. Shirai, S. Yuasa, Y. Suzuki, Recent progress in the voltage-controlled magnetic anisotropy

effect and the challenges faced in developing voltage-torque MRAM. Micromachines (Basel) (2019). https://doi.org/10.3390/mi10050327

92. M. Weisheit, S. Fähler, A. Marty, Y. Souche, C. Poinsignon, D. Givord, Electric field-induced modification of magnetism in thin-film ferromagnets. Science **1979**(315), 349–351 (2007)
93. T. Nan, Z. Zhou, M. Liu, X. Yang, Y. Gao, B.A. Assaf, H. Lin, S. Velu, X. Wang, H. Luo, J. Chen, S. Akhtar, E. Hu, R. Rajiv, K. Krishnan, S. Sreedhar, D. Heiman, B.M. Howe, G.J. Brown, N.X. Sun, Quantification of strain and charge co-mediated magnetoelectric coupling on ultra-thin permalloy/PMN-PT interface. Sci. Rep. **4**, 3688 (2014)
94. A. Begué, M. Ciria, Strain-mediated giant magnetoelectric coupling in a crystalline multiferroic heterostructure. ACS Appl. Mater. Interfaces **13**, 6778–6784 (2021)
95. Y. Deng, Y. Yu, Y. Song, J. Zhang, N.Z. Wang, Z. Sun, Y. Yi, Y.Z. Wu, S. Wu, J. Zhu, J. Wang, X.H. Chen, Y. Zhang, Gate-tunable room-temperature ferromagnetism in two-dimensional Fe3GeTe2. Nature **563**, 94–99 (2018)
96. T. Li, S. Jiang, N. Sivadas, Z. Wang, Y. Xu, D. Weber, J.E. Goldberger, K. Watanabe, T. Taniguchi, C.J. Fennie, K. Fai Mak, J. Shan, Pressure-controlled interlayer magnetism in atomically thin CrI3. Nat. Mater. **18**, 1303–1308 (2019)
97. B. Xu, S. Li, K. Jiang, J. Yin, Z. Liu, Y. Cheng, W. Zhong, Switching of the magnetic anisotropy via strain in two dimensional multiferroic materials: CrSX (X = Cl, Br, I). Appl. Phys. Lett. **116**, 052403 (2020)
98. H. J. M. Swagten, K. H. J. Buschow, Handbook of magnetic materials (2007)
99. F. Huang, M.T. Kief, G.J. Mankey, R.F. Willis, Magnetism in the few-monolayers limit: a surface magneto-optic Kerr-effect study of the magnetic behavior of ultrathin films of Co, Ni, and Co–Ni alloys on Cu(100) and Cu(111). Phys. Rev. B **49**, 3962–3971 (1994)
100. H.-J. Elmers, J. Hauschild, U. Gradmann, Critical behavior of the uniaxial ferromagnetic monolayer Fe(110) on W(110). Phys. Rev. B **54**, 15224–15233 (1996)
101. C.A.F. Vaz, J.A.C. Bland, G. Lauhoff, Magnetism in ultrathin film structures. Rep. Prog. Phys. **71**, 056501 (2008)
102. T. Song, X. Cai, M.W.-Y. Tu, X. Zhang, B. Huang, N.P. Wilson, K.L. Seyler, L. Zhu, T. Taniguchi, K. Watanabe, M.A. McGuire, D.H. Cobden, D. Xiao, W. Yao, X. Xu, Giant tunneling magnetoresistance in spin-filter van der Waals heterostructures. Science **1979**(360), 1214–1218 (2018)
103. Z. Wang, D. Sapkota, T. Taniguchi, K. Watanabe, D. Mandrus, A.F. Morpurgo, Tunneling spin valves based on Fe_3GeTe_2/hBN/Fe_3GeTe_2 van der Waals heterostructures. Nano Lett. **18**, 4303–4308 (2018)
104. W. Zhu, H. Lin, F. Yan, C. Hu, Z. Wang, L. Zhao, Y. Deng, Z.R. Kudrynskyi, T. Zhou, Z.D. Kovalyuk, Y. Zheng, A. Patanè, I. Žutić, S. Li, H. Zheng, K. Wang, Large tunneling magnetoresistance in van der Waals ferromagnet/semiconductor heterojunctions. Adv. Mater. **33**, 2104658 (2021)
105. W. Zhu, S. Xie, H. Lin, G. Zhang, H. Wu, T. Hu, Z. Wang, X. Zhang, J. Xu, Y. Wang, Y. Zheng, F. Yan, J. Zhang, L. Zhao, A. Patanè, J. Zhang, H. Chang, K. Wang, Large room-temperature magnetoresistance in van der Waals ferromagnet/semiconductor junctions. Chin. Phys. Lett. **39**, 128501 (2022)
106. W. Zhu, Y. Zhu, T. Zhou, X. Zhang, H. Lin, Q. Cui, F. Yan, Z. Wang, Y. Deng, H. Yang, L. Zhao, I. Žutić, K.D. Belashchenko, K. Wang, Large and tunable magnetoresistance in van der Waals ferromagnet/semiconductor junctions. Nat. Commun. **14**, 5371 (2023)
107. T. Scheike, Z. Wen, H. Sukegawa, S. Mitani, 631% room temperature tunnel magnetoresistance with large oscillation effect in CoFe/MgO/CoFe(001) junctions. Appl. Phys. Lett. **122**, 112404 (2023)
108. W. Jin, G. Zhang, H. Wu, L. Yang, W. Zhang, H. Chang, Room-temperature spin-valve devices based on Fe3GaTe2/MoS2/Fe3GaTe2 2D van der Waals heterojunctions. Nanoscale **15**, 5371–5378 (2023)
109. H. Yin, P. Zhang, W. Jin, B. Di, H. Wu, G. Zhang, W. Zhang, H. Chang, Fe_3GaTe_2/$MoSe_2$ ferromagnet/semiconductor 2D van der Waals heterojunction for room-temperature spin-valve devices. CrystEngComm **25**, 1339–1346 (2023)
110. W. Zhu, S. Xie, H. Lin, G. Zhang, H. Wu, T. Hu, Z. Wang, X. Zhang, J. Xu, Y. Wang, Y. Zheng, F. Yan, J. Zhang, L. Zhao, A. Patané, J. Zhang, H. Chang, K. Wang, Large room-temperature magnetoresistance in van der Waals ferromagnet/semiconductor junctions. Chin. Phys. Lett. **39**, 128501 (2022)
111. W. Jin, G. Zhang, H. Wu, L. Yang, W. Zhang, H. Chang, Room-temperature and tunable tunneling magnetoresistance in Fe_3GaTe_2-based 2D van der Waals heterojunctions. ACS Appl. Mater. Interfaces **15**, 36519–36526 (2023)

Publisher's Note Springer Nature remains neutral with regard to jurisdictional claims in published maps and institutional affiliations.